Advanced International Journal of Material Science and Engineering
Volume.8, Number 1; January-March, 2023;
ISSN: 2837-3928 | Impact Factor: 8.26
http://zapjournals.com/Journals/index.php/aijmse
Published By: Zendo Academic Publishing

TOWARDS SUSTAINABILITY: AGRO-WASTE REINFORCED ALUMINIUM COMPOSITES

Ngozi Chinyere Okonkwo[1] and Ibrahim Usman Abdullahi[2]

Article Info

Keywords: Aluminium matrix composites, Hybrid composites, Reinforcements, Agrowastes, Mechanical properties

Abstract

The utilization of aluminium matrix composites (AMCs) has experienced significant growth in various industrial applications owing to their exceptional combination of high strength, low density, durability, machinability, availability, and cost-effectiveness. These unique properties render AMCs highly attractive for lightweight applications, including automotive, aerospace, military, and transportation sectors, due to their high specific strengths, excellent fatigue properties, and wear resistance. To further enhance the scope of these desirable properties, researchers have explored the concept of hybrid aluminium matrix composites (HAMCs), achieved through the incorporation of hard and lightweight micro or nano particles as reinforcements. Widely used reinforcement materials include silicon carbides (SiC), titanium borides (TiB2), alumina (Al2O3), nitrides, boron, and graphite.

In recent studies, the application of agrowastes as reinforcements in AMCs has gained attention. Agrowastes such as rice waste ash, sugar cane bagasse, palm kernel ash, periwinkle shell ash, and coconut shell ash have been investigated as potential cost-effective and readily available alternatives. Notably, the addition of these agro-waste reinforcements has shown promising results in enhancing the mechanical properties of AMCs.

This research work focuses on the preparation and characterization of hybrid AA6061 alloy composites by incorporating silicon carbide (SiC) and carbonized coconut shell particles into the matrix using the stir casting method. The effectiveness of these reinforcements in improving the mechanical characteristics of the resulting composites, including tensile strength, impact strength, and hardness, will be evaluated and compared with other commonly used reinforcements like fly ash.

In a similar context, other researchers have explored different reinforcement materials, such as aloe vera powder and cow horn

[1] University of Uyo, Nigeria

particulates, and investigated their impact on the mechanical properties of aluminium metal matrix composites. The utilization of artificial neural networks (ANN) and response surface methodology (RSM) for modeling the age hardening process in reinforced AMCs has shown promising outcomes, resulting in enhanced predictions and understanding of the composite behavior.
Additionally, this work investigates the density, porosity, microstructure, and mechanical properties of particulate periwinkle shell-aluminium 6063 metal matrix composites (PPS-AlMMCs). The two-step casting technique was employed to produce these composites with varying filler loadings. The results reveal the uniform distribution of the filler within the matrix and its influence on the composite's density, porosity, strength, ductility, hardness, and modulus.
Overall, this study aims to contribute to the expanding knowledge base on innovative reinforcements for AMCs, exploring the potential of agrowastes and other unconventional materials to further enhance the performance and applicability of aluminium matrix composites in diverse engineering applications.

INTRODUCTION

The application of aluminium matrix composites (AMC) in industrial practice in recent times has grown tremendously because of their good combination of high strength, low density, durability, machinability, availability, and its comparatively low materials cost. Thus, they are very attractive for lightweight applications such as automobile, aerospace, military and transport sectors due to high specific strengths, good fatigue properties and wear resistance (Wang et al., 2014; Karl, 2006). The scope of these properties can be extended by singly or multiply reinforced aluminium matrix with hard and light micro or nano particles leading to the formation of hybrid aluminium matrix composites (HAMCs), (Parswajinan et al., 2018; Sudipt and Ananda, 2008; Michael et al., 2015). The property of the AMCs depends on the property of the matrix and the reinforcement (Vijaya et al., 2014). The reinforcement in AMCs may be in the structure of continuous fibres, discontinuous fibres, whiskers or particulates. Widely used reinforcement ceramic materials in AMCs include silicon carbides (SiC), titanium borides (TiB_2), alumina (Al_2O_3), nitrides, boron and graphite.

Recently, reinforcements commonly used in aluminium matrix composites have been extended to include agrowastes such as rice waste ash, sugar cane bagasse, palm kernel ash, periwinkle shell ash and coconut shell ash (Senthilkumar et al., 2016; Iyasele, 2018). These agro-wastes are cheap and readily available in high quantity. Ajibola and Fakeye (2015) reported the production and characterization of Zinc-Aluminium composite reinforced with silicon carbide and palm kernel shell ash (PKSA), in which samples prepared with compositions 5wt% SiC added with 0.2%, 0.4%, 0.6%, 0.8% and 1.0wt% PKSA were utilized to prepare the reinforcing phase with Zinc-Aluminium matrix composite using two step stir casting method. The agro waste material was preheated to 650^{o}C before being introduced into the Zinc-Aluminium composite in molten state. Hardness and tensile test were used to characterize the composite produced. The result shows that increase in PKSA reinforcement increases the hardness and tensile strength of the composite, and the microstructure shows that SiC and PKSA were well dispersed in the alloy matrix.

Hima et al., (2018) used aloe vera powder to reinforce the aluminum metal matrix in order to study the mechanical characteristics of the AMC. He compared the suitability of fly ash (reported by several researchers) and aloe vera

as reinforcement particulates for the aluminum metal matrix, but his study reported that the use of aloe vera significantly reflected an improvement on the mechanical properties of the AMC with regards to tensile strength, impact strength, and hardness, compared to the popularly known and used fly ash. Nwobi-Okoye and Ochieze (2018) experimentally studied the behavior of aluminum alloy A356 reinforced with a particulate composite of cow horn, for application in a brake drum via the use of an artificial neural network (ANN), response surface methodology (RSM), and simulated annealing. The study was focused on modeling the age hardening process on the developed or reinforced AMMC using ANN and RSM. The result revealed that the modeling via ANN that generated the data for age hardening was improved by 0.9583 predictions compared with that of RSM of 0.9921 predictions of ANN.

Umunakwe et al., (2017) investigated the density, porosity, microstructure and some mechanical properties of particulate periwinkle shell-aluminium 6063 metal matrix composite (PPS-AlMMC) produced by two-step casting and compared the properties of the composites with those of the aluminium 6063 (Al60603) alloy. Periwinkle shells were milled to particle sizes of 75µm and 150µm and used to produce PPS-AlMMC at 1, 5, 10 and 15wt% filler loadings using two-step casting technique. The addition of PPS to aluminium alloy reduced the density of the composite. It was observed that the filler distributes uniformly in the matrix due to the two-step casting technique. The porosities of the composites were within acceptable level of 0-5% except for the composite with 15wt% PPS of 150µm particle size. Improved strength, ductility, hardness and modulus were obtained when the filler was used to reinforce the alloy. However, using a filler of higher particle size resulted to higher porosity, reduced tensile strength, ductility and toughness.

In this work, attempt has been made to prepare and characterize hybrid AA6061 alloy composites by adding SiC and carbonized coconut shell reinforcement particles into the matrix using stir casting method

MATERIALS AND METHODS

The various materials used for this study includes aluminium alloy 6061, silicon carbide and coconut shell. Table 1 shows the chemical composition of Al6061 Alloy. The coconut shells were washed, dried and carbonized at 600^{o}C for 5 hours. Both the carbonized coconut shell and silicon carbide particulates were ball milled for 60 hours and 50 hours respectively in accordance with the work of Bello (2017). After milling, the reinforcement particulates were classified for particle size. Samples of the AA6061/SiC/CCS composites were then fabricated by stir casting method at 700^{o}C using a crucible (Figure 1e), with addition of 2wt% Magnesium to enhance the wettability between reinforcements and molten metal. The molten metal was stirred using a stainless steel stirrer and measured quantity of reinforcement (0, 3, 6, 9, 12 and 15%wt of equal mixtures of CCS and SiC respectively with different particle sizes) was added. The mixture was stirred for 5 minutes for uniform distribution. Then molten metal was poured in a sand mould and allowed to solidify.

Table 1: Composition of AA6061

Element	Si	Fe	Cu	Mn	Mg	Ni	Zn	Ti	Cr	Al
Weight (%)	0.514	0.230	0.161	0.071	0.960	0.010	0.015	0.031	0.103	Bal.

Figure 1: (a) Coconut shells (b) Silicon carbide (c) Cast AA6061 ingot (d) Crushed carbonized coconut shells (e) Carbonized coconut particulates (f) Stir casting furnace

Density Measurements

Density measurements were carried out on the developed composite samples using Archimedes' principle. The samples were first weighed in air and then weighed when fully immersed in water. The difference in mass of each sample was recorded and used to calculate the density of the sample. The experimental density of composite was thus calculated using Equation 1.

$$\rho_{cexp} = \frac{W_{air}}{W_{air} - W_{water}} \times \rho_{water} \quad (1)$$

where, W_{air} is the weight of composite in air, W_{water} the weight of composite in water and ρ_{water} the density of composite in water

Hardness Testing

The hardness of the aluminium alloy and composites were determined with Vicker's hardness tester (Figure 2a). The dimension of each specimen for hardness testing was diameter 30mm × 15mm thick (Figure 1b) and each specimen was grinded and polished to obtain a flat smooth surface. During the testing, a load of 980.7N was applied for 10s on the specimen through square based pyramid indenter and the hardness reading taken in a standard manner. The readings were taken in two different points at the surface of the hardness specimen and the average computed as the hardness of the specimen.

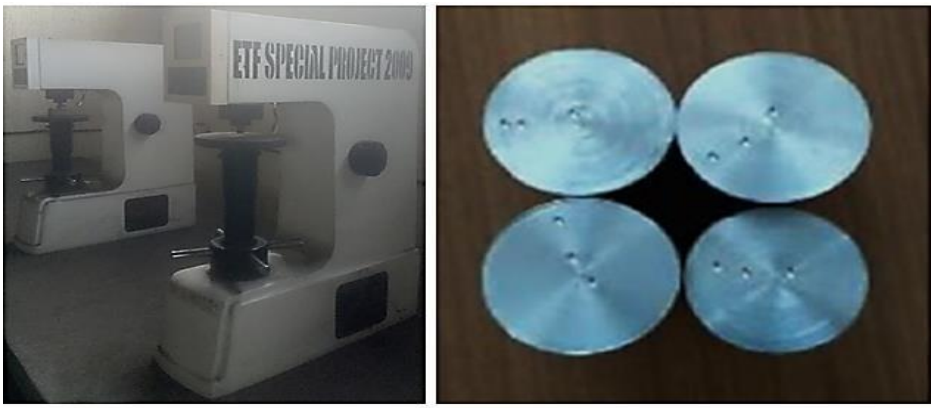

(a) Testing machine (b) Test specimens

Figure 2: Hardness test

Tensile testing

The tensile test was carried out on the composite samples to determine its strength and ductility, yield strength and other tensile properties. In the present investigation all the tensile tests were conducted using Monsanto Tensometer {type W, serial 11148} tensile test machine in the Department of Metallurgical and Materials Engineering, Federal University of Technology, Owerri. The standard tensile test sample of a dumbbell shape with a diameter of 6.5 mm and gauge length 28 mm was used for the research. An initial load of 5kN was applied on the samples, with the load increased until failure occurred. The specimen was axially loaded in tension; the distance between the gauge marks was monitored. The specimen was elongated by the moving crosshead, load cell and extensometer measured the magnitude of the load and the elongation. All tests were conducted at room temperature.

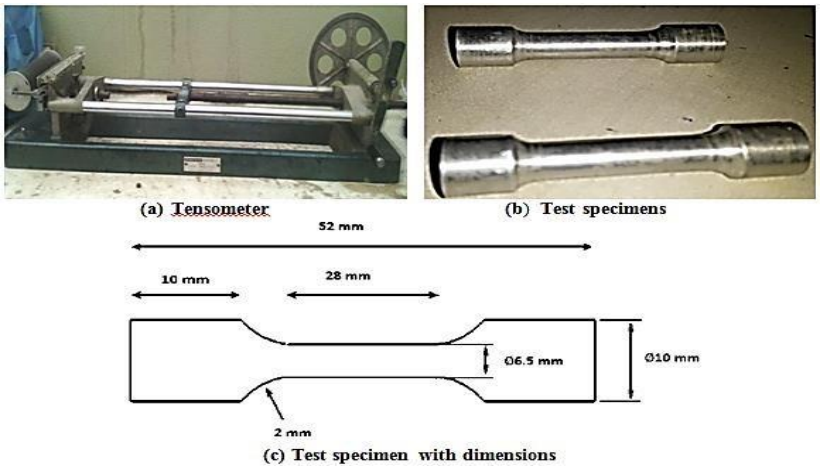

Figure 3: Tensile test set up

Modeling Tensile strength

In the current study the aluminum matrix is assumed to be an elastic-plastic material and the inclusions are approximated as being made of spherical and linear-elastic silicon carbide and carbonized coconut shell particulates. The interface between the matrix and the inclusions assumed to be ideal and particle cracking is not considered. Analytical model established by Punkanszky et al., (1988) gives an empirical relationship between strength of composite (σ_c) and strength of matrix (σ_m) as given in Equation 2.

$$\sigma_c = \sigma_m \frac{1-V_p}{1+2.5V_p} e^{BV_p} \quad [(\quad)] \tag{2}$$

where, an empirical constant B is dependent on particle surface area, interfacial bonding strength, and particle density. The B value varies in between 3.49 to 3.87. The Punkanzky empirical relationship as given in Equation 1, gives the ultimate strength of the particulate metal matrix composite which depended on the strong particlematrix interfacial bonding. Also, considering adhesion, precipitate formation, particle size, agglomeration, voids/porosity, dislocation obstacles and the particle/matrix interfacial reaction, modified Voigt model considering these factors may be expressed as;

$$\left.\begin{aligned} \bar{\sigma_c} &= V_m\bar{\sigma}_m + \sum V_{r_j}\bar{\sigma}_{r_j} + \varepsilon_f \\ \bar{\varepsilon_c} &= V_m\bar{\varepsilon}_m + \sum V_r\,\bar{\varepsilon}_r + \varepsilon_f \end{aligned}\right\} \{j = 1,2,\dots,n\} \tag{3}$$

where $\bar{\sigma_c}$, $\bar{\sigma_m}$ and $\bar{\sigma_{rj}}$ are the composite, matrix and reinforcement strength respectively and $\bar{\varepsilon_c}$, $\bar{\varepsilon_m}$ and $\bar{\varepsilon_{rj}}$ are the corresponding strains. The volume fractions of matrix material and reinforcement are respectively, $_m$ and V_{rj}. The term ε_f, is a correction factor accounting for the effect of reinforcement particle size, porosity and interfacial

interaction, and was determined from experimental data of the composite. In this study, the matrix material is reinforced with two different types of particulates, thus Equation 3 is rewritten as

$$\left.\begin{aligned}\bar{\sigma_c} &= V_m\bar{\sigma}_m + V_{r_1}\bar{\sigma}_{r_1} + V_{r_2}\bar{\sigma}_{r_2} + \varepsilon_f\\ \bar{\varepsilon_c} &= V_m\bar{\varepsilon}_m + V_{r_1}\bar{\varepsilon}_{r_1} + V_{r_2}\bar{\varepsilon}_{r_2} + \varepsilon_f\end{aligned}\right\} \quad (4)$$

$$\text{But } {}_m + V_{r1} + V_{r2} = 1 \qquad \Rightarrow V_m = 1 - (V_{r1} + V_{r2})$$

where, V_m, V_{r1} and V_{r2} are the volume fractions of the matrix and the two different particulates 1 and 2 respectively.

The modified load transfer effect according to Sanaty-Zadeh (2012) is given as;

$$\Delta\sigma_{LT} = \frac{1}{2}V_p\sigma_m \quad (5)$$

and the Hall-Petch strengthening equation as modified by Hull and Bacon (2001) is;

$$\Delta\sigma_{H-P} = \frac{k_y}{\bar{d}} \quad (6)$$

√

Combining Equations 4 and 5, and neglecting the volume fractions of voids/porosity gives Equation 7.

k

$$\sigma_c = \frac{1}{2}V_p\sigma_m + \frac{y}{\sqrt{d_p}} \quad (7)$$

For matrix material reinforced with n different particulates, Equation 7 becomes,

$$\sigma_c = \frac{1}{2}\left(\sum V_{p_i}\right)\sigma_m + \frac{k_y}{\sqrt{\left(\sum d_{p_i}\right)}} \quad \{i = 1, 2, n\} \quad (8)$$

For matrix material reinforced with two different particulates, Equation 8 becomes

$$\sigma_c = \frac{1}{2}\left(V_{p_1} + V_{p_2}\right)\sigma_m + \frac{k_y}{\sqrt{\left(d_{p_1} + d_{p_2}\right)}} \quad (9)$$

Table 2 gives the material data for models prediction.

Table 2: Material and model parameters

Material	Elastic modulus (GPa)	Tensile strength (MPa)	Density (g/cm^3)	Poisson ratio
Silicon carbide particles	410	336	3.21	0.14
Carbonized coconut shell particles	512	18.03	1.68	0.92
AA6061	69	162.6	2.72	0.33

RESULTS AND DISCUSSION Chemical composition of Reinforcements

The results obtained from the XRF chemical compositional analysis of the carbonized coconut shell particles (CCSp) and SiC shown in Tables 3, revealed that the carbonized coconut particulates contained SiO_2, MgO, Al_2O_3 and Fe_2O_3 in great amount with small amounts of CaO, K_2O, Na_2O, MnO and ZnO. The presence of hard substances like SiO_2, Al_2O_3 and Fe_2O_3 suggest that the carbonized coconut shell particles can be used as particulate reinforcement in various metal matrix composites (Apasi et al., 2016; Madakson et al., 2012). This result is consistent with the results by Donald et al., (2018), Apasi et al., (2016) and Madakson et al., (2012), and the chemical composition has similarity with the XRF analysis of periwinkle shell ash, rice husk ash, fly ash and bagasse ash currently used in metal matrix composite as reported by Nwabufoh (2015), Hassan and Aigbodion (2010) and Rajan et al., (2007). Therefore, the present work suggests the suitability of carbonized coconut shell as particulates reinforcement in metal matrix composites.

Table 3: Chemical composition of Reinforcements

CCS									
Element	Al_2O_3	CaO	Fe_2O_3	K_2O	MgO	Na_2O	SiO_2	MnO	ZnO
%	16.50	0.58	14.50	0.51	16.51	0.50	46.70	0.42	0.35
SiC									
Element	SiC	Si	SiO_2	Fe	Al	C			
%	98.6	0.30	0.6	0.09	0.10	0.3			

Density of composites

The results of the experimental density of the alloy and composites reinforced with micro and nano-particulates of SiC and CCS are shown in Table 4. Addition of reinforcement particles to the matrix alloy has significant effect on the composite density.

Table 4: Densities of composites

%wt. of reinforcement	Density (g/cm^3)								
	AA6061 with								
	µSiC	µCCS	n_fSiC	n_SSiC	n_fCCS	n_SCCS	μSiC/μCCS	n_fSiC/n_fCCS	n_SSiC/n_SCCS
0	2.72	2.72	2.72	2.72	2.72	2.72	2.72	2.72	2.72
3	2.75	2.67	2.74	2.75	2.56	2.60	2.70	2.65	2.67
6	2.80	2.54	2.77	2.79	2.47	2.50	2.68	2.63	2.65
9	2.84	2.50	2.80	2.82	2.43	2.47	2.65	2.61	2.62
12	2.87	2.42	2.83	2.85	2.30	2.38	2.64	2.57	2.60
15	2.91	2.37	2.86	2.90	2.09	2.21	2.62	2.49	2.53

n_fSiC: First nano SiCp (42.3nm) n_SSiC: Second nano SiCp (55.8nm) µSiC: SiC micro-particles (38µm) n_fCCS: First nano CCSp (50.01nm) n_SCCS: Second nano CCSp (60.3nm) µCCS: CCS micro-particles (63µm)

Table 4 indicates that addition of micro and nano particles of SiC increased the composite density beyond that of the matrix alloy, whereas, the composite density decreased upon addition of micro and nano particulates of coconut shell. The observed increase in composite density may be caused by the higher density of SiC (3.21g/cm^3) as compared with that of the base alloy. The decrease in density associated with the use of CCS particles is caused by the lower density of CCS (1.68g/cm^3) compared to the density of aluminium matrix which is 2,72 g/cm^3, oxidation of the base alloy, gas evolution and porosity in the composites. These results are consistent with earlier work of Prasad (2006) and Abba-Aji (2021). Table 4 also indicates that the density of nano-composites decreased with both increasing weight fraction and decreasing particle size. Notably, the use of CCS nanoparticles further decreased the composite density. Peter et al. (2020) reported similar observation with the use of CCS in spark plasma sintered Ti-Ni based metal matrix composite. The density of the developed AA6061/n_fCCS and AA6061/n_SCCS composites reduced by 23.2% and 18.75% on addition of 15wt.% each of n_fCCS and n_SCCS respectively, whereas that of the AA6061/nSiC composites increased by 5.2% and 6.62% on addition of 15wt.% each of n_fSiC and n_SSiC, respectively. Note that two different categories of nanocomposites were presented for each reinforcement; first SiC nano-composites (AA6061/n_fSiC), second SiC nano-composites (AA6061/n_sSiC), first CCS nano-composites (AA6061/n_fCCS) and second CCS (AA6061/n_SCCS). The trend of experimental density values obtained therefore indicates that the first CCS nanocomposites (AA6061/n_fCCS) acquired lowest densities. For the hybrid composite, densities were significantly reduced below that of the matrix

alloy upon addition of combined micro and nano particulates of SiC and CCS. The composite density decreased by 0.74%, 2.6% and 1.84% at 3wt.% addition of μSiC/μCCS, n_fSiC/n_fCCS and n_sSiC/n_sCCS, respectively. Figure 4 shows the comparative density plots of the different composites produced. It indicates that maximum and minimum densities were achieved with composites singly reinforced with μSiC and nCCS respectively. The observed order of decrease in density were with; μSiC/μCCS, nSiC/nCCS, μCCS and nCCS, respectively. The composite densities also increased in the order, μSiC and nSiC. Hence it is evident that the CCS particulates reduced the composite density whereas the SiC particulates increased the composite density. Similar trend were reported by Donald et al.,(2018) and Padmavathi and Ramakrishnan (2019). This result trend therefore indicates that the hybrid AA6061/nSiC/nCCS composites will be better suited for light weight applications. Note that nSiC, nCCS and nSiC/nCCS in Figure 4 represent average response for n_fSiC and n_sSiC; n_fCCS and n_sCCS; n_fSiC/n_fCCS and n_sSiC/n_sCCS respectively.

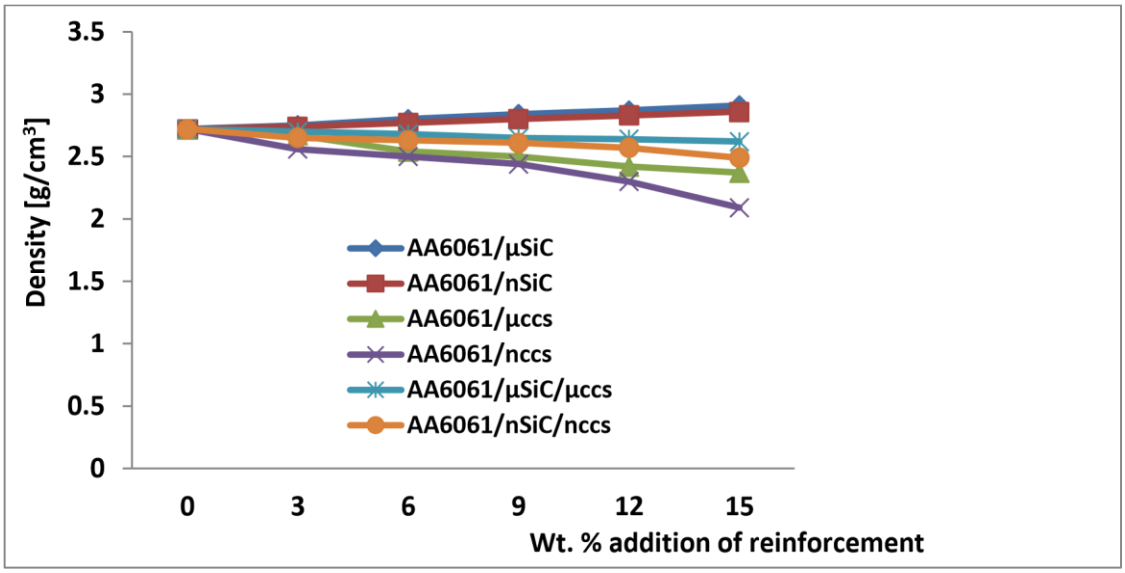

Figure 4: Comparative plots of the aluminium alloy 6061 composite densities Hardness of Composites

The average hardness values of the matrix alloy and composites reinforced with different weight percent and particle sizes of SiC and CCS are presented in Table 5. The composite hardness values were observed to increase with increasing weight percent and decreasing particle size of reinforcements.

Table 5: Average hardness of composites

%wt. of reinforcement	Hardness (HV) AA6061 with								
	µSiC	µCCS	n_fSiC	n_sSiC	n_fCCS	n_sCCS	μSiC/μCCS	n_fSiC/n_fCCS	n_sSiC/n_sCCS
0	78.8	78.8	78.8	78.8	78.8	78.8	78.8	78.8	78.8
3	80.0	79.2	83.0	81.6	80.0	79.1	81.0	85.3	83.5
6	82.0	80.8	84.5	83.5	83.1	82.0	84.1	87.0	85.0
9	84.2	83.1	85.7	85.0	84.0	83.2	85.8	88.6	86.9
12	86.0	84.0	88.0	86.2	85.6	85.0	88.6	92.2	89.4
15	87.0	84.8	90.0	87.4	86.3	85.7	90.0	95.0	92.0

n_fSiC: First nano SiCp (42.3nm) n_sSiC: Second nano SiCp (55.8nm) µSiC: SiC micro-particles (38µm) n_fCCS: First nano CCSp (50.01nm) n_sCCS: Second nano CCSp (60.3nm) µCCS: CCS micro-particles (63µm)

The composite hardness value increased by 2.79%, 8.25% and 5.97% with 3wt.% addition of μSiC/μCCS, n_fSiC/n_fCCS and n_sSiC/n_sCCS, respectively. The composite hardness further increased by 14.21%, 20.55% and 16.75% with 15wt.% addition of μSiC/μCCS, n_fSiC/n_fCCS and n_sSiC/n_sCCS, respectively. Maximum hardness values were achieved with addition of n_fSiC particulates. The observed increase in hardness value is attributed to the matrix phase refinement and the integration of hard and brittle phases of micro and nano- particles of silicon carbide (μSiC and nSiC), SiO_2, Al_2O_3 and Fe_2O_3 (obtained from carbonized coconut shell particulates) in the matrix material. Similar trend has been reported in literature (Ajibola and Fakeye, 2015; Hima et al., 2018; Bello, 2017). Umunakwe et al., (2017) also reported the increase in hardness of composite reinforced with 75µm particulate size over those reinforced with and 150µm particulate size. It is believed that the decrease in particle size enhanced interfacial excellent bond, increased dislocation density and thus improved hardness and strength. Notably, SiC reinforced composites acquired superior hardness compared with those reinforced with CCS. This is because SiC has higher hardness value than CCS. Compared with the hybrid micro composites (AA6061/$\boldsymbol{\mu}$SiC/$\boldsymbol{\mu}$CCS), the hybrid nano composites (AA6061/nSiC/nCCS) possessed superior hardness. This is caused by further particle size reduction and higher bond strength between the nanoparticles and the matrix alloy.

Modeling of Hardness of Hybrid AA6061/SiC/CCS nano composites

The effects of reinforcement weight percent (Wt) on the hardness of AA6061/nSiC/nCCS composites was appraised using a linear model developed for theoretical prediction of the hardness (response) with percent weight, W_t as predictor. Therefore, this model involves 5 different levels and two predictors (5^1) equivalent to 5 experimental runs using balanced two – factor factorial design of experiment. Table 6 reveals the experimental design, actual, predicted and residual hardness. Functions derived for the model revealed in Equations 10 and 11. The adequacy and validity of the developed model was tested through ANOVA as shown in Tables 7 and 8 The model has a p – value of 0.000 which is < 0.05 (i.e. $\alpha = 0.05$ or 95% confidence) and F – value of 241.938 indicating that the model is considered to be statistically significant. The significant model terms are considered to generate the model and are identified with p values < 0.05. However, model terms with p value > 0.05 are regarded as insignificant. The difference between the predicted R^2(0.984) and adjusted R^2(0.980) is within the acceptable limit < 0.2 in order to establish a reasonable agreement.

$$\text{Hardness} = \beta_0 + \beta_1(\text{Wt})^{\text{n}} \tag{10}$$

with $\beta_0 = 77.9, \beta_1 = 178.67$ and $\text{n} = 1$, the model equation becomes

$$\text{Hardness} = 77.9 + 178.67(\text{Wt\% nSiC/nCCSp}) \tag{11}$$

Table 6: Comparison of measured and modeled hardness of hybrid nano composites

Order	Predictor Wt.% (nSiC+nCCS)	Response Hardness (Hv)		
		Measured	Model	Residual
1	3	89.2	88.62	−0.58
2	6	93.0	99.34	6.34
3	9	117.3	110.06	−7.24
4	12	123.0	120.78	−2.22
5	15	127.8	131.50	3.70

Table 7: Test for significance of nSiC/nCCS composites Hardness

Order	Predictor	Unstandardized β	Standard error	Standardized β	t	Significance	Tolerance	VIF
1	Constant	77.90	1.719		44.669	0.000		
2	Wt % CCSp/SiC	178.67	0.189	0.992	15.554	0.000	1.000	1.000

Dependent Variable: Hardness VIF: Variance inflation factor

Table 8: Test result of ANOVA for nSiC/nCCS composites Hardness

Source	Sum of squares	Degree of freedom (df)	Mean square	P value	(F-value)	Predicted R^2	Adjusted R^2	
		1				0.984	0.980	Model
Regression	1364.897	1	1364.897	0.000	241.938			
		4	5.642					Residual
		22.566						

Comparative plots of measured and model predicted composite hardness values are given in Figure 5.
It indicates deviation of model predictions from measured data, with minimum and maximum deviations of 0.65% at 3wt. % addition of nSiC/nCCS and 6.17% at 9wt. % addition of nSiC/nCCS respectively. The observed deviations of model predicted values from experimental results are believed to be caused by non-inclusion of effect of other process parameters such as mould/melt interactions, agglomeration, porosity, stirring speed, pouring temperature in model development.

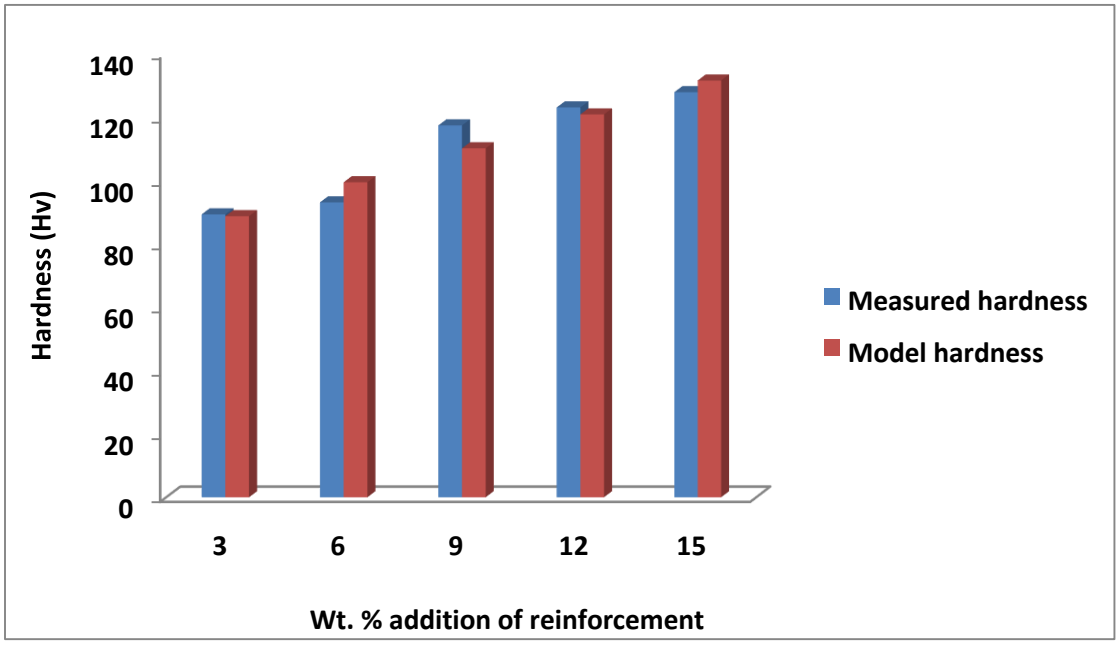

Figure 5: Hardness values of hybrid nano-composite

Tensile and Yield strength of Hybrid AA6061/SiC/CCS Composites

Figure 6 depicts progressive improvement in ultimate tensile and yield strength values for hybrid micro and nano composites. The ultimate tensile and yield strengths of the composites were observed to continuously improve as the percentage of the particles was increased. This improvement continues with decreasing reinforcement particulate size. This is evident as the hybrid nano-composites acquired superior ultimate tensile and yield strengths than the hybrid micro-composites. Similar trend has been reported in literature (Prasad and Krishna, 2010; Abba-Aji, 2021; Michael, 2022). Donald et al.,(2018) and Padmavathi and Ramakrishnan (2019) also reported improved tensile strength properties of AMC composite. The observed increase in strength value is attributed to the matrix phase refinement and the integration of hard and brittle phases of micro and nano- particles of silicon carbide (μSiC and nSiC), SiO_2, Al_2O_3 and Fe_2O_3 (obtained from micro and nano- particles of carbonized coconut shell; μCCS and nCCS) in the matrix material. The hard and brittle phases constitute barriers to dislocation movement across the grain boundaries. This in effect strengthens the soft matrix and improves the composites hardness. Another factor that may contribute to the better interaction between the particles and the matrix is the clean and clear interface between them, conferring the composite an increased load-carrying capacity. Composites with 15wt.% nSiC/nCCS and 15wt.% μSiC/μ/CCS presented maximum improvement in ultimate tensile strength value (53.4% and 41.5% respectively, for nSiC/nCCS and μSiC/μ/CCS) compared to the base alloy. Another possible reason for the improved ultimate tensile strength value could be the interaction between the particles and dislocations when the composites are under load; could also be due to the existence of several appending dislocations around the particles owing to the variation in the thermal expansion coefficient between the particles and the base matrix. The mismatch in thermal expansion coefficient between the matrix and the particles will also strengthen dislocation at the grain boundary based on the level of mismatch. The increase in yield strength was due to the decreased inter-particle spacing between the SiC and CCS particles as the particles are harder than the base alloy. Also, the addition of micro and nano particulates of SiC and CCS to the base alloy suppressed stress deformation, thereby improving the yield strength of the composites.

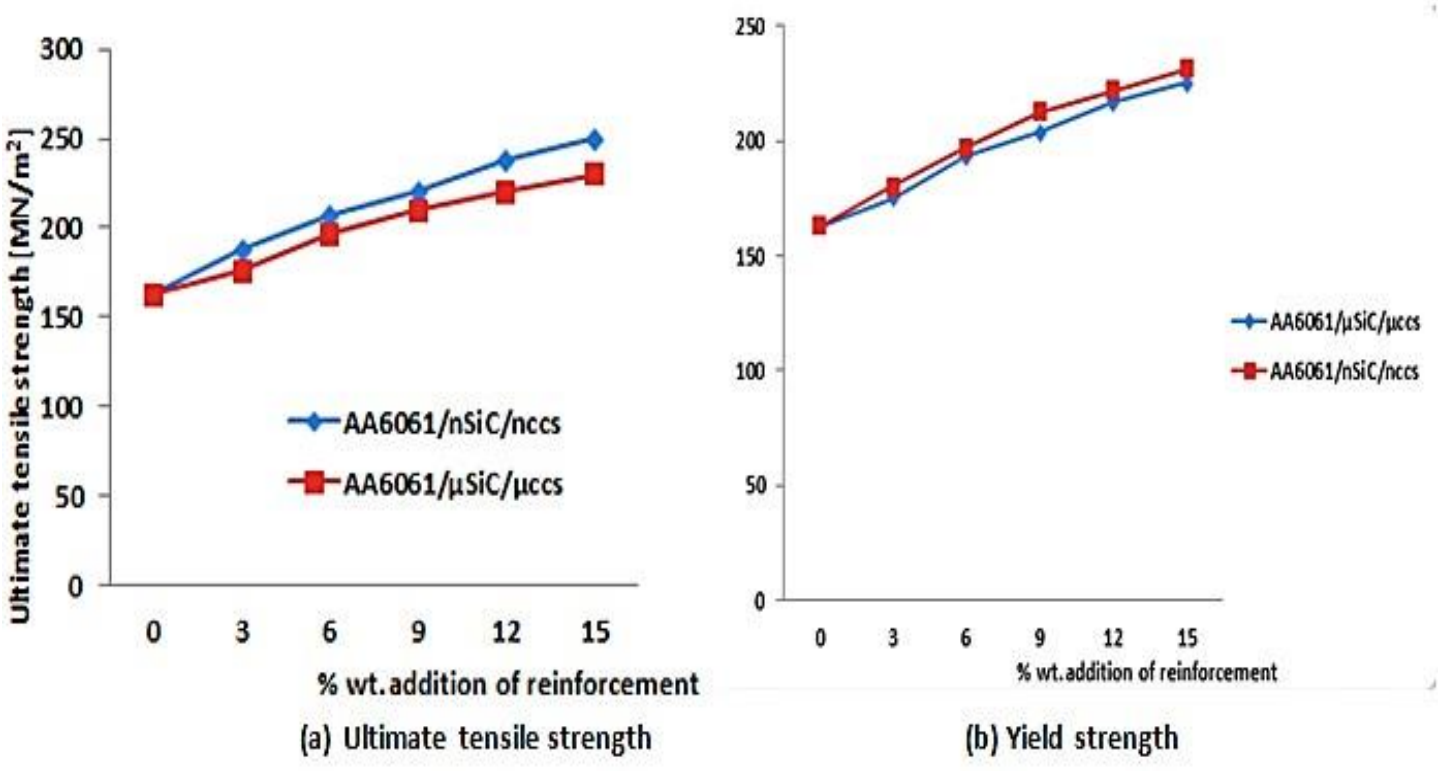

Figure 6: Variation of the strengths of Hybrid AA6061/SiC/CCS micro and nano composites with reinforcement additions

Modeling of Tensile Strength of hybrid AA6061/SiC/CCS nano composites

The experimental data for composite strength, accompanied by mathematical model predictions from earlier works and present study are shown in Table 9 and Figure 7. Widely used models for the prediction of composite strength and the proposed model are listed in Table 10. Table 9 and Figure 7 indicates that the results of the predictions by the proposed model in this work are in excellent agreement with those of the experimental data, Voigt's model and Punkankzy's model and thus validates it suitability for tensile strength prediction of particle reinforced hybrid metal matrix composites. Further, it was observed that the popular Voigt's model gives significantly higher values than the measured values and those by Reddy and the present work. This is because the Voigt's model does not take into account the effect of reinforcement particle size, porosity and interfacial reactions in the composite. However, a modified Voigt model was developed by introducing a correction factor that accounts for the effect of particle size, porosity and interfacial interactions that was determined from the experimental data of the composite. Hence the results of the modified Voigt model given in Table 9 are consistent with those of the experimental data, Punkankzy's model as well as the proposed model.

Table 9: Comparison of Experimental and Model predicted composite strengths for the Al6061 composites

S/N	Wt.% of nSiC and nCCS	Measured σ_c (MPa)	Modified Voigt's model		Punkankzy's model		Proposed model	
			Predicted σ_c (MPa)	Residuals σ_c (MPa)	Predicted σ_c (MPa)	Residuals σ_c (MPa)	Predicted σ_c (MPa)	Residuals σ_c (MPa)
1	3	187.5	187.51	0.01	187.60	0.10	187.34	− 0.16
2	6	207.0	206.90	− 0.10	207.20	0.20	207.12	− 0.12
3	9	220.1	220.10	0.00	220.14	0.04	220.09	− 0.01
4	12	238.0	237.90	− 0.10	238.04	0.04	238.28	0.28
5	15	249.5	250.00	0.50	249.40	− 0.10	249.68	0.18

The value of strength constant k_y for the proposed model (see Table 10) as determined from experimental data ranges from 3.92×10^{-3}MPa (at 6wt.% addition of nSiC and nCCS) to 4.48×10^{-3}MPa (at 30wt.% addition of nSiC and nCCS) while the correction factor for the modified Voigt's model ranges from 24.04 to 82.58 MPa for reinforcement addition ranging from 6wt. % to 30 wt. % addition of nSiC and nCCS. Also the B value in Punkankzy's model varies in between 4.48 to 5.74 in decreasing amount of reinforcement addition in contrast with the stated range of 3.49 to 3.87 as given by Punkankzy. The variation in B values compared with those of Punkankzy was attributed to non-inclusion of effect of precipitate formation, agglomeration, voids/porosity and dislocation barriers in the response computation.

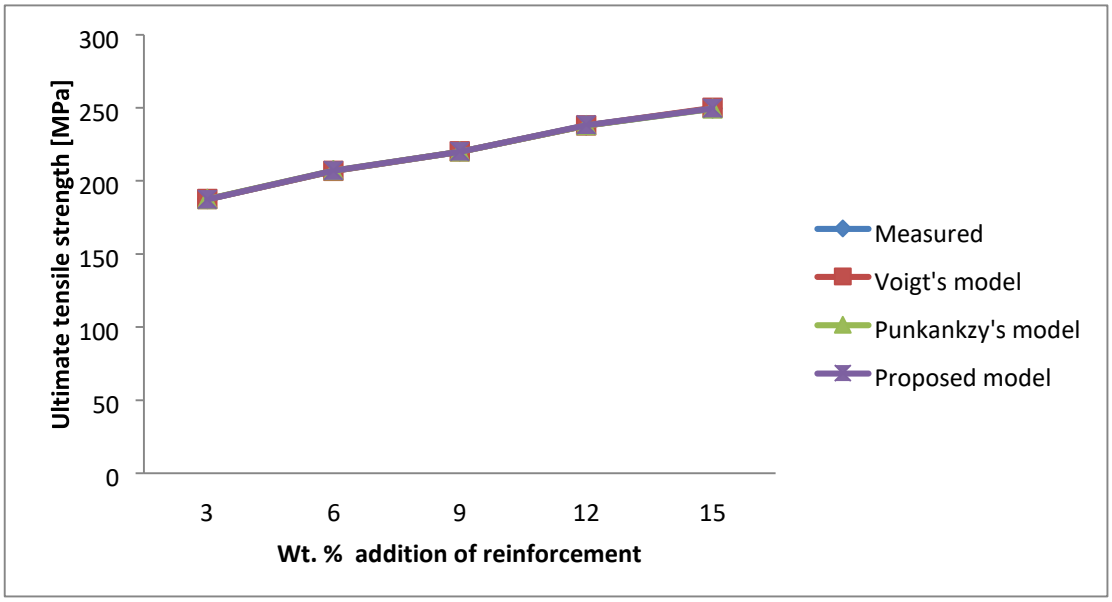

Figure 7: Comparative plots of hybrid nano-composite strength obtained from model prediction

Table 10: Models for prediction of composite strength

S/N	Author(s)	Model	Equation
1	Voigt	$\sigma_c = V_m\bar{\sigma_m} + \sum V_{rj}\bar{\sigma_{rj}} + \varepsilon_f \quad \{j = 1,2, \dots, n\}$	3
2	Punkankzy	$\sigma_c = \left[\sigma_m\left(\frac{1-(\sum V_{p_i})}{1+2.5(\sum V_{p_i})}\right)\right] e^{B(\sum V_{p_i})} \quad \{i = 1,2,n\}$	2
3	Present work	$\sigma_c = \frac{1}{2}(\sum V_{p_i})\sigma_m + \frac{k_y}{\sqrt{(\sum d_{p_i})}} \quad \{i = 1,2,n\}$	7

However, comparative analysis of the composite strength precisely obtained from experiment and predictive models shows that the model- predicted values, deviated from experimental results as presented in Figure 5. The maximum tolerable deviations (residuals) of model predictions from experimental data were 0.2%, 0.1% and 0.12% for Voigt's model, Punkankzy's model and the proposed model respectively. The observed deviations are caused by the effect of other process parameters such as stirring speed, stirring temperature, particle agglomeration, melt/mould interactions (reactions) etc. which were ignored during the model development and evaluations. It can therefore be concluded that the proposed model is suitable for prediction of tensile strength of nano-particulate composites with some modifications. The modifications may be the introduction of error factor that will account for the various process parameters affecting the measured response (strength), which can be determined from experimental data for nanocomposite composition.

Microstructure of Hybrid AA6061/nSiC/nCCS Composites

The SEM micrographs of the AA6061 alloy and those of the composites are shown in Figure 8. Figure 8(a) shows the micrograph of the unreinforced alloy revealing the white α −phase with equiaxed grain shape (Boppana et al., 2020). Fine grains are found along grain boundaries as far as possible in the structure of AA6061 alloy. The result of SEM for microstructural examination of the specimens revealed fairly uniform distribution of nSiC and nCCS in the matrix in all %wt addition of the reinforcements (Figure 8b-d).

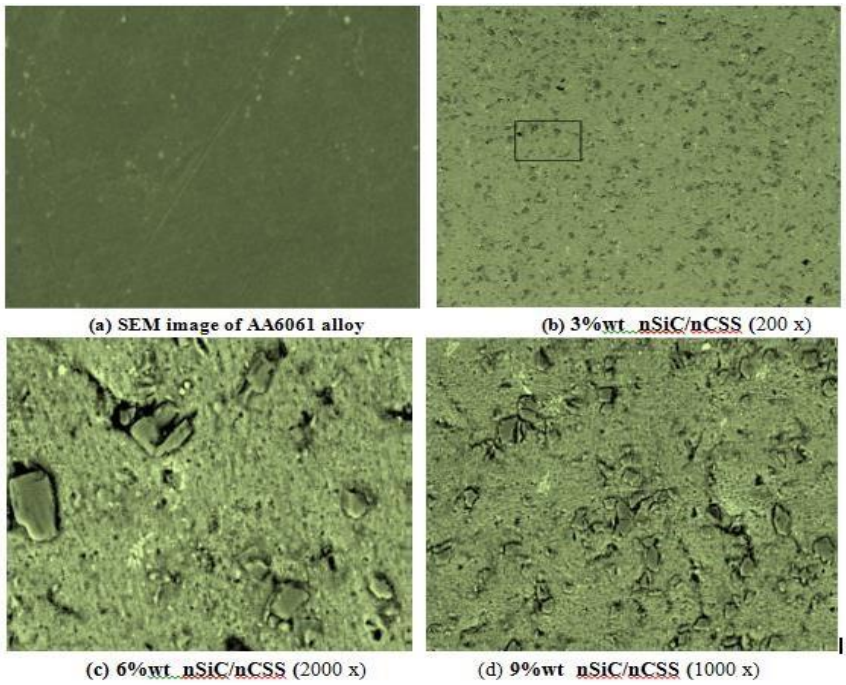

Figure 8: SEM images of hybrid AA 6061/nSiC/nCCS composites

The uniform distribution of nSiC and nCCS particles in the matrix can be attributed to a number of factors which includes, effective stirring of the melt, degassing tablet used and good wettability that resulted in improved interfacial bonding between the matrix and the coconut shell ash particles (Apasi et al., 2016).No segregation of nSiC and nCCS particles were found along the grain boundaries. Distribution of particles was observed to be intra-granular, in which the majority of the particles locate inside the grains. This distribution is preferred in AMCs to have better mechanical and tribological properties. Silicon carbide and carbonized coconut nanoparticles were thermodynamically stable, and there were no pores or voids around them. The reinforcement particles resisted aluminium grain growth and resulted in nucleation sites growth, which led to the formation of finer grains. As the concentration of nSiC and nCCS particles increased in the matrix, composite properties such as hardness, UTS, and resistance to wear also showed improvement.

CONCLUSION

The hybrid AA6061/SiC/CCS composites have been successfully produced by stir casting method and characterized for analysis of density, hardness, strength and microstructural properties. The effect of reinforcement particulates size and volume fraction on the properties of the AA6061/SiC/CCS composites were also investigated. From the analysis of results obtained during this study, the following conclusions were made:

1. The incorporation of the silicon carbide and coconut shell particulates into the aluminium alloy matrix decreased the density but increased the hardness, ultimate tensile and yield strength values of the composites
2. The hybrid AA6061/SiC/CCS nano-composites acquired superior hardness and tensile strength properties with least density when compared with the hybrid micro-composite and the matrix alloy.
3. The nano-particulates reinforced composite presented maximum improvement in ultimate tensile strength value (53.4% of that the unreinforced matrix) at reinforcement level of 15wt.% nSiC/nCCS.
4. The microstructure analysis of the composites revealed a uniform distribution of the reinforcement particles in the matrix. This resulted in excellent bonding properties and grain refinement.

5. The composites can be used in areas where higher strength to weight ratio is required within the aerospace, automotive and electronic industries such as cylinder liners in engines, aluminuim calipers and power electronic modules.

References

Abba-Aji, M. A. (2021), Development of Car Piston Material from Aluminium alloy using Coconut shell ash as an additive. PhD Thesis, Department of Industrial and Production Engineering, Federal University of Technology, Minna, Nigeria

Ajibola, W.A. and Fakeye, A.B. (2015), Production and Characterization of Zinc- Aluminium, Silicon Carbide Reinforced with Palm Kernel Shell Ash, Int. J. Eng. Trends and Tech. (IJETT), 41(6), 318 – 325.

Apasi, A., Yawas, D. S., Abdulkareem, S. and Kolawole, M. Y. (2016), Improving Mechanical Properties of Aluminium Alloy Through Addition of Coconut Shell-Ash, Journal of Science and Technology, 36(3), 34-43

Bello Sefiu Adekunle (2017) Development and Characterisation of Epoxy-Aluminium-Coconut shell particulate hybrid nanocomposite for automobile applications, PhD Thesis, Department of Metallurgical and Materials Engineering, University of Lagos, Nigeria.

Boppana, S. B., Dayanand, S., Kumar, A., Kumar, V. and Aravinda, T (2020). Synthesis and characterization of Nano graphene and ZrO_2 reinforced AA6061 metal matrix composites.

J. Mater. Res. Technol. 2020, 9, 7354–7362.

Donald, A.O., Hassan, M.A., Hamza, S., Garba, E., Dangtim, D.K. and Mamadou, M. (2018), Development and Characterization of Aluminum Matrix Composites Reinforced with Carbonized Coconut Shell and Silicon Carbide Particle for Automobile Piston Application, Global Scientific Journals, 6(8), 390 – 398.

Hassan, S.B. and Aigbodion, V.S. (2010), The study of the Microstructure and Interfacial Reaction of Al-Cu Mg/Bagasse Ash Particulate Composite, Journal of Alloy& Compounds, 491: 571–574. Hima, G. C., Durga P. K. G., Ramji, K. and Vinay, P. V. (2018), Mechanical Characterization of Aluminium Metal Matrix Composite Reinforced with Aloe vera powder, Mater. Today, 5, 3289–3297. Hull, D and Bacon, D.T. (2001), Introduction to Dislocations, 4th Edition; Butterworth Einmemann; Oxford, U.K.

Iyasele, E. Omondiale (208), Comparative Analysis On The Mechanical Properties Of A Metal- Matrix Composite (Mmc) Reinforced With Palm Kernel/Periwinkle Shell Ash, Global Sc. J., 6(8) 1 – 24.

Karl, U. Kainer, (2006) Metal Matrix Composites. Custom-made Materials for Automotive and Aerospace Engineering, WILEY-VCH Verlag GmbH & Co. KGaA, Weinheim.

Madakson, P. B., Aigbondon, V. S., Apasi, and Yawas, D. S. (2012). Wear behaviour of AlSi-Fe alloy/coconut shell ash particulate composites, Tribology in industry, 34(1): 36 -43.

Michael, O. B., Kenneth, K. A. and Lesley, C. (2015), Aluminium matrix hybrid composites: A review of reinforcement philosophies; mechanical, corrosion and tribological characteristics, J. Mater. Research and Technol., 4(4) 434–445.

Michael, N. Nwigbo (2022), Synthesis and Characterization of Hybrid Aluminium Matrix Composites Reinforced with Silicon Carbide and Carbonized Coconut Shell Particulates for Automotive Applications, PhD Thesis, Department of Mechanical and Aerospace Engineering, University of Uyo, Nigeria.

Nwabufoh Michael N. (2015), Development and Characterization of Al-3.7%Cu-1.4%Mg Alloy/Periwinkle Ash (Turritella Communis) Particulate Composites, M.Eng. Thesis, Department of Metallurgical and Materials Engineering, Ahmadu Bello University, Nigeria.

Nwobi-Okoye, C. C. and Ochieze, B. Q. (2018), Age hardening process modeling and optimization of Aluminium alloy A356/Cow horn particulate composite for brake drum application using RSM, ANN and simulated annealing. Def. Technol., 14, 336–345

Padmavathi and Ramakrishnan (2019), Wear Studies on the Heat Treated Al6061-μSiC and Al6061-nSiC Metal Matrix Composites, Intl. J. Mech. Engg and Tech., (10) 6, 241-247.

Parswajinan, C., Vijaya, B. R., Abishe, B., Niharishsagar, B. and Sridhar, G. (2018), Hardness and impact behaviour of aluminium metal matrix composite, The 3rd International Conference on Materials and Manufacturing Engineering 2018, IOP Conf. Series: Materials Science and Engineering 390 (2018) 012075.

Prasad, N. (2006), Development and characterization or metal matrix composite using red Mud an industrial waste for wear resistant application, PhD thesis Department of Mechanical Engineering, National Institue of Technology Rourkcla -769 008 (India) January, pp 23-34.

Rajan, T.P.D, Pillai, R.M, Pai B.C, Satyanaryana, K.G, and Rohatgi P.K, (2007), Fabrication and characterization of Al-7Si-0.35Mg/fly ash metal matrix composites processed by different stir casting routes, Composites Science and Technology, pp 67,3369-3377.

Sanaty-Zadeh, A. (2012), Comparison between current models for the strength of particulate- reinforced metal matrix nanocomposites with emphasis on consideration of Hall–Petch effect. Mat. Sci. Eng. A, 531, 112–118.

Senthilkumar, G., Manoharan, S., Balasubramanian, K. and Dhanasakkaravarthi, B. (2016), An Experimental Investigation of Metal Matrix Composites of Aluminium (Lm6), Boron carbide and Fly ash, Australian Journal of Basic and Applied Sciences, Vol. 10(1), 137-144.

Sudipt Kumar and Ananda Theerthan J. (2008), Production and Characterisation of Aluminium- Fly Ash Composite Using Stir Casting Method, B. Tech. Project, Department of Metallurgical & Materials Engineering National Institute of Technology, Rourkela.

Umunakwe, R., Olaleye, D. J., Oyetunji, A., Okoye, O. C. and Umunakwe, I. J. (2017), Assessment of the Density and Mechanical Properties of Particulate Periwinkle Shell- Aluminium 6063 Metal Matrix Composite (PPS-AlMMC) Produced by Two-Step Casting, ACTA TECHNICA CORVINIENSIS – Bulletin of Engineering Tome X [2017] Fascicule 1 [January – March].

Vijaya, R. B., Elanchezhian, C., Annamalai, R. M., Aravind, Sri Ananda, A. S. T., V. Vignesh, V. and Subramanian, C. (2014), Aluminium Metal Matrix Composites - A Review, Rev. Adv. Mater. Sci. 38(2014) 55 – 60.

Wang, Z., Prashanth, K.G., Scudino, S., Chaubey, A.K., Sordelet, D.J., Zhang, W.W., Li, Y.Y. and Eckert, J. (2014). Tensile properties of Al matrix composites reinforced with in situ $Al_{84}Gd_6Ni_7Co_3$ glassy particles. J. Alloy. Compd. 2014, 586, S419–S422.